THERAPEUTIC ADVANCES in
Musculoskeletal Disease

Review

Advanced imaging techniques in crystal arthritis

Ther Adv Musculoskelet Dis

2025, Vol. 17: 1–15

DOI: 10.1177/1759720X251316097

Victor Laurent, Georgios Filippou, Silvia Sirotti and Tristan Pascart

***Abstract*:** Gout and calcium pyrophosphate deposition (CPPD) disease are the most common causes of crystal arthritis. Identifying the pathogenic crystal deposition is the cornerstone of the diagnosis, but also prognosis and monitoring of the diseases. Conventional radiography has been for decades the only imaging technique used, with its very restricted sensitivity in both diseases. Advanced techniques, namely ultrasound and dual-energy computed tomography (DECT), are being increasingly used in the diagnosis and management of gout and CPPD diseases, and their role is now well recognized in classification criteria and in recommendations for the diagnosis and management. In gout, ultrasound elementary lesions of monosodium urate deposition are well defined and have been shown to be sensitive to change and can be monitored, while direct quantification of these deposits can be performed with DECT. In CPPD disease, the definition of elementary lesions and their scoring has been well established for ultrasound, while the proof of concept that DECT can help discriminate calcium pyrophosphate crystal deposits among other calcium-containing structures has been shown. The aim of this narrative review is to provide an overview of the use of advanced imaging techniques in crystal-induced arthropathies.

Keywords: calcium pyrophosphate deposition, dual-energy computed tomography, gout, ultrasound

Received: 23 July 2024; revised manuscript accepted: 10 January 2025.

Introduction

Crystal-induced arthropathies share similar patterns of inflammation directly triggered by the abnormal presence of crystals in joints and periarticular structures. Gout, caused by monosodium urate (MSU) crystals, and calcium pyrophosphate deposition (CPPD) disease are the most common crystal-induced arthropathies.[1,2] While polarized light microscopy remains the gold standard for crystal identification, imaging holds a central role in diagnosing and monitoring crystal-induced arthropathies, as well as for assessing inflammation and evaluating structural damage in affected joints.[3]

Conventional radiography was for a long time the only available technique. It was barely useful and nonspecific for the first attack of gout, while it had good specificity but a relatively poor sensitivity for CPPD.[4] The development of "advanced" imaging techniques, namely ultrasound (US)[5] and dual-energy computed tomography (DECT),[6] opened up new prospects for the diagnosis and management of crystal arthritis, including being able to provide noninvasive evidence of crystals, as recently acknowledged by EULAR recommendations on imaging of crystal-induced arthropathies.[3] Imaging not only refines the diagnosis of crystal arthritis but is also considered in the prognosis of diseases, as well as in their management.[3]

The aim of this narrative review is to provide an overview of the use of advanced imaging techniques in crystal-induced arthropathies. The focus was deliberately made on US and DECT, which were the only techniques included in the American College of Rheumatology (ACR)/European Alliance of Associations for Rheumatology (EULAR) classification criteria for gout and CPPD, and in 2023 EULAR imaging recommendations, leaving aside magnetic

Correspondence to:
Tristan Pascart
Service de Rhumatologie, Hôpital Saint-Philibert, Lille Catholic University, rue du Grand But, Lomme, Lille 59160, France
pascart.tristan@ghicl.net

Victor Laurent
Department of Rheumatology, Saint-Philibert Hospital, ETHICS Laboratory, Lille Catholic University, Lille, France

Georgios Filippou
Rheumatology Department, IRCCS Istituto Ortopedico Galeazzi, Milan, Italy

Department of Biomedical and Clinical Sciences, University of Milan, Milan, Italy

Silvia Sirotti
Rheumatology Department, IRCCS Istituto Ortopedico Galeazzi, Milano, Italy

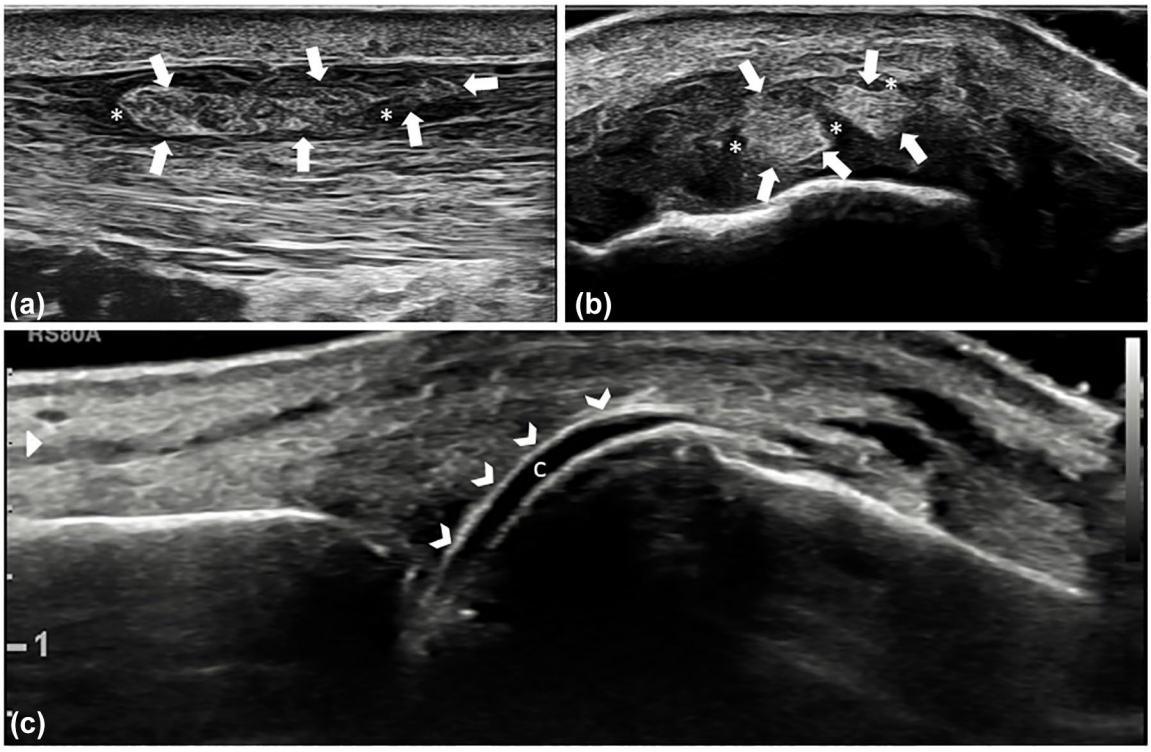

Figure 1. Ultrasonographic lesions of gout. (a) An intratendinous tophus of the Achilles tendon and in (b) intracapsular tophi of the first metatarsophalangeal (MTP) joint (arrows). Tophi may present any degree of echogenicity and may also create posterior acoustic shadowing. A typical US characteristic of a tophus is the presence of a hypoechoic halo (asterisks) that reflects inflammatory process around the crystal deposition. In (c), the typical appearance of the double contour sign in a metacarpal-phalangeal joint, which is a continuous hyperechogenic line (arrowheads) covering the surface of the hyaline cartilage (c) even where the US is not perpendicular on the cartilage like in the deeper part of the metacarpal head.
US, ultrasound.

resonance imaging, which is of limited specificity in crystal-induced arthropathies.[1–3]

Gout

Ultrasound use and elementary lesions in gout

The gold standard for the diagnosis of gout remains the identification of MSU crystals by synovial fluid aspiration, which is not always feasible. The OMERACT US working group has been working for the last 10 years to validate US as a tool for the assessment of gout, starting by providing definitions of four US elementary lesions of MSU deposits: double contour (DC), tophi, aggregates, and bone erosions (Figure 1). The DC sign is defined as an abnormal hyperechoic band over the superficial margin of the articular hyaline cartilage which may be either irregular or regular, continuous or intermittent and can be distinguished from the cartilage interface sign. Tophus is defined as a circumscribed, inhomogeneous, hyperechoic, and/or hypoechoic aggregation, which may be surrounded by a small anechoic rim. Gout aggregates are defined as bright hyperechoic, isolated spots too small to fulfill the tophus definition, and characterized by maintaining their high degree of reflectivity when the insonation angle is changed.[7] Finally, erosions are intra- and/or extra-articular discontinuity of bone surface, visible in two perpendicular planes.[8] Inter-reader reliability was found to be good for tophus and erosions, fair for DC, but low for aggregates (κ 0.21, 95% confidence interval (CI) 0.04–0.37).[9] MSU deposits may have more variable echogenicity (from hypoechoic to hyperechoic) than calcium pyrophosphate (CPP) crystals. They are frequently inhomogeneous and may generate posterior acoustic shadowing, and the images are often not as typical as what is

classically shown in atlases.[10] Changing the angle of insonation and reducing the gain level hardly influence the appearance of very hyperechogenic MSU deposits.[10] At a low level of gain, both MSU deposits and bone, which are highly hyperechoic, remain identifiable, while other causes of hyperechoic abnormalities (debris, synovial proliferation, and other soft tissue interfaces) tend to become undistinguishable.[10] Identification of crystals using US is not so easy, and training is necessary to avoid pitfalls.

Diagnostic performances of US

US appears to have high sensitivity and specificity for detecting MSU deposits. A systematic literature review with meta-analysis assessed the diagnostic performance of US in about 4000 joints and nearly 3000 tendons and cartilage areas of gout and control patients and found a pooled sensitivity and specificity reaching, respectively, 65.1% and 89.0% to detect MSU deposits.[11] Presence of US Tophi is very specific of gout (93.2%), but has a rather low sensitivity (54.3%).[11] The DC sign generally offers a higher sensitivity but suffers from questionable reliability as its diagnostic accuracy depends on joint shape and size. The DC sign results from the enhancement of the chondro-synovial margin, which appears thicker than normal. Synovial fluid collection will falsely overestimate the normal chondro-synovial interface in the presence of overlying fluid collections and need to be cautiously considered. In the systematic literature review for EULAR recommendations, the majority of studies assessing the usefulness of US in diagnosing gout found a sensitivity and specificity of $\geqslant$80%.[12] When looking specifically at individual features, the DC sign had a sensitivity of $\geqslant$80% in only about one-third of the studies and was very specific, so that a definite identification of the DC sign can be considered sufficient for the diagnosis of gout when synovial fluid analysis is not available.[3,12]

Monitoring MSU crystal deposition in ULT

US is increasingly used to monitor patients, as change in elementary lesions seems to be associated with clinical response.[13,14] The OMERACT working group had followed-up a group of 50 patients during their first 6 months of urate lowering therapy (ULT) and showed that US elementary lesions were sensitive to change, except for erosions.[15] In patients initiating ULT followed-up using US in a multicenter study, US showed a greater decrease in tophus size and the DC sign with a low SU level, with DC sign disappearance evidenced earlier during ULT therapy.[16] After 3 months of ULT, half of the joints examined in patients with an SU level $<$5.0 mg/dl showed that the DC sign had disappeared, and tophus size reduction was significant after 6 months of efficient ULT therapy. In addition, a 50% decrease in tophus size after 6 months of ULT is predictive of a lower flare risk after stopping prophylactic treatment.[17] The decrease in tophus size and the DC sign disappearance was greater with a low SU level ($<$5.0 mg/dl) compared to an SU level between 5 and 6.0 mg/dl.[16] The OMERACT working group developed a semiquantitative scoring system to capture the extent the size of MSU deposits and refine the assessment of their debulking during treatment.[18] In the NOR-GOUT study including 209 patients receiving treat-to-target ULT with sequential US scans using a semiquantitative scoring system of 0–3 of elementary lesions (DC, tophi, and aggregates), treatment resulted in significant reductions of all the depositions and of the semiquantitative score, most extensively for DC.[19] These data suggest that US could be a useful tool in the follow-up of gout as it is able to monitor the MSU crystal depletion during ULT and could improve the concept of treat-to-target therapy in gout. What is more, it could help the physician to personalize care by discontinuing flare prophylaxis at an appropriate time to avoid flare-ups after treatment is discontinued.

Detection of MSU deposits beyond joints

The pathogenic role of MSU crystal deposition in the renal medulla, known as gout nephropathy, is debated in patients with gout. In an US study, the presence of frequent hyperechoic medulla suggestive of crystal deposition has been reported in severe tophaceous gout patients.[20] In this study, Bardin et al.[20] found that these hyperechoic renal lesions were associated with renal dysfunction and features of tubulo-interstitial nephritis in 502 patients and tended to decrease with ULT. Further studies are needed to confirm this hypothesis.

What's recommended for the use of US in gout?

In 2023, EULAR issued recommendations on imaging for the diagnosis and management of crystal-induced arthropathies, advising US as the first-line imaging modality in gout, and supporting scanning symptomatic areas and specific target sites (first MTP joint).[3] When characteristics

of MSU crystal deposition are present on US (DC sign, tophus), 2023 EULAR recommendations were the first to support that synovial fluid analysis is not needed to confirm a diagnosis of gout in patients with a typical clinical picture. The relevance of monitoring gout with imaging needed to be demonstrated through further studies to be formerly recommended, but the task force underlined that it could help to show some infra-clinical inflammation, as well as the DC sign, tophi, and aggregates, shown to be sensitive to change, which could help for follow-up. There is evidence that assessing the amount of MSU crystal deposition with US could be used to predict future flares, and US will no doubt be involved in managing flare prophylaxis in the near future.[16] Finally, US is useful to guide synovial fluid aspiration based on anatomical landmarks when aspiration is challenging, and it can be useful to help explain the disease to patients to improve their understanding of the disease and contribute to better treatment adherence.[3]

A brief reminder of how DECT works and the basic principles of its application to gout

The use of DECT in gout is based on the principle that the attenuation of tissues, reflected by their CT attenuation in Hounsfield units (HU), depends on their density as well as their atomic number (Z) and the energy photon beam. DECT uses two photon spectra of low and high energies, each attenuated by the studied tissue. Postprocessing algorithms combine the attenuations of these two energy beams to identify the biochemical composition of each voxel.[21] In gout, DECT uses the fact that MSU crystal deposits increase the density of the soft tissue they are in, without any photoelectric effect. MSU crystals, therefore, attenuate the two energy beams in a similar way, but increase the density of the tissue[22] (Figure 2). The addition of all voxels considered to contain MSU then provides a quantitative measurement of the volume of MSU crystals deposited (Figure 3).

DECT is unable to identify intra-articular MSU crystal deposition (except in rare cases of large intra-articular tophi) and has no equivalent to the US DC sign. DECT will identify MSU deposits in soft tissue surrounding joints and in tendons, whether or not organized in tophi. The measurement of tophi with DECT provides smaller volumes than with US, as the latter measures the tophus as a whole (including the cellular envelope of the tophus), while DECT measures only the crystal core.[23]

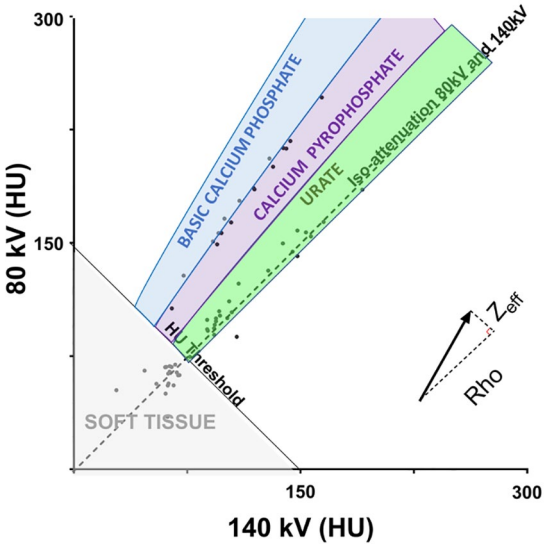

Figure 2. Principle of MSU coding by postprocessing software of DECT scans. Combined effects of volumetric mass density (Rho) and effective atomic number (Z_{eff}) on CT numbers at 80 and 140 kV for tophi. Each dot representing a combined value of attenuations at 140 and 80 kV will be coded as MSU (green box) if situated above the cut-off line and around the line where attenuations at both energies are equal. Dots below the cut-off line will be coded as soft tissue, and dots above the bow will be coded as calcium pyrophosphate (purple box) or basic calcium phosphate.
DECT, dual-energy computed tomography; HU, Hounsfield unit; MSU, monosodium urate.

Artifacts and pitfalls when using DECT for gout

Postprocessing settings are decisive in ensuring that MSU-coded lesions appear on DECT. Most DECT artifacts are now well known as they can be misidentified for MSU (nails, skin thickening, tendon reflection, bone surfaces, and degenerative menisci), and some attempts are made to optimize settings to avoid these misleading images before assessing total MSU volume.[24,25] In addition, DECT parameters depend on the type of machine used and its brand. Most of the published literature contains reports of studies using Siemens® (Healthineers, Erlangen, Germany) and, to a lesser extent, Philips® (Healthcare, Andover, United-States), General Electrics® (Healthcare, Chicago, United-States), and Canon® (Healthcare, Otawara, Japan) machines, and it is still largely unknown whether results from a certain type of machine can be reproduced on another. To avoid false positivity,

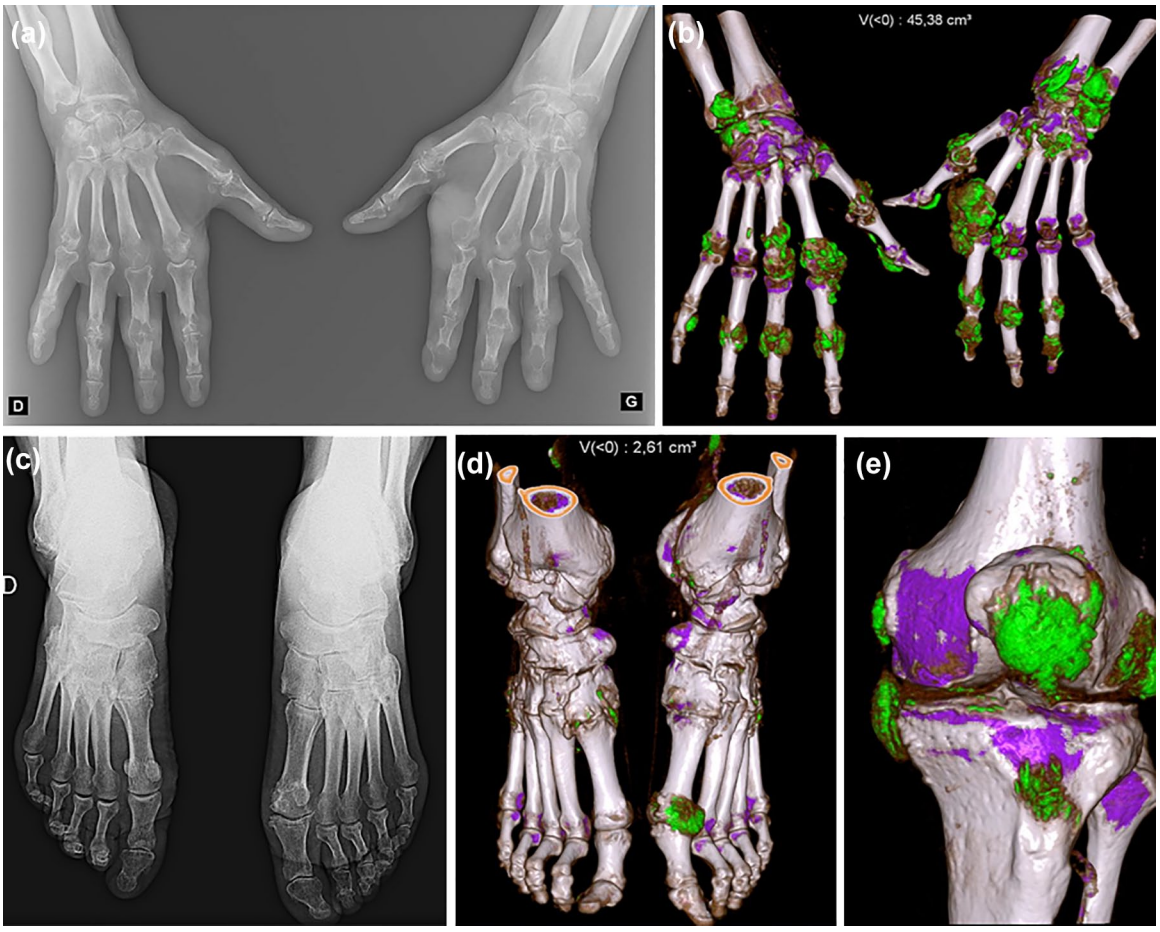

Figure 3. Typical DECT images of patients with tophaceous and erosive gout. Conventional radiographs (a) and DECT scans (b) of the hands of an early 60s-year-old man with tophaceous and erosive gout. Conventional radiographs (c) and DECT scans of the feet (d) and DECT scans of the knees (e) of a 58 year-old patient with tophaceous gout. DECT images were obtained using the "gout" mode postprocessing settings (Siemens SyngoVia).
DECT, dual-energy computed tomography.

submillimeter lesions should not be taken into account,[26,27] and considering only global volumes above 0.1 cm^3 seems more reliable than the 0.01 cm^3 threshold.[28] There is no current consensus over what a negative DECT scan for MSU crystal deposition is, and the specificity (and sensitivity) of the device depends on the chosen settings of the postprocessing software.[29] In default settings, 1-mm lesions are usually considered artifactual and some known artifacts need to be removed manually by the reader (e.g., nail beds), but the minimal global volume above which the reader can confidently assume that some of the volume at least is genuinely composed of MSU crystals is unclear. Some studies suggest that the conventional threshold of 0.01 cm^3 commonly admitted as artifactual is probably not sufficiently specific to avoid artifacts, with a higher threshold of 0.1 cm^3 appearing to be more specific and correlated to clinical and US assessments (SU level, DC sign on US), which suggest frequent false positives with the 0.01-cm^3 threshold. Patients with $<0.1\,cm^3$ of MSU crystals may tend to flare less throughout the 2 years after initiating ULT but this has yet to be confirmed by further studies.[28] Results suggests that gout patients with $<0.1\,cm^3$ MSU deposits are not associated with any particularly prolonged inflammatory activity in terms of reaching SU level targets, similar ULT doses required, and no prolonged flare prophylaxis.

Diagnostic performances

The first studies examining the diagnostic performances of DECT in gout were conducted in established diseases, which led to an overestimation of the sensitivity of DECT in detecting MSU crystal

deposits.[6,30] Several studies have reported the systematic assessment of gout patients with both DECT and ultrasound,[31] showing for the most part variable results due to inconsistent methodology and lack of standardization leading to various center-dependent results. One group performed a pooled meta-analysis showing that DECT detection of MSU deposits was overall superior to ultrasound in terms of sensitivity (89% vs 84%) and specificity (91% vs 84%) when both the ultrasound DC sign and tophi were included in the assessment.[32]

DECT use is recent in gout disease and provides substantial knowledge to understand the physiopathology of gout and improve medical care through indirect evidence of crystals. In terms of diagnosis, DECT is particularly useful in atypical presentations of gout posing a diagnostic challenge and distinguishes gout from other arthropathies, particularly in cases when joint aspiration is not feasible. DECT is fully recognized in the diagnostic setting of gout, including by the latest 2023 EULAR recommendations for imaging of crystal arthropathies,[2,33] and the prognostic value of DECT in predicting the risk of flares and comorbidity onset is being actively explored.[34,35]

One study looked at comparative and combined performances of systematic scanning of knees and ankles/feet both with DECT and US in 147 patients, the results of which favored the performance of DECT over US, mainly because of the questionable reliability of the DC sign in the first MTP. Combining the two techniques did not provide significant improvement in diagnostic performances over DECT alone. However, combining the techniques could improve the negative predictive value to ascertain the absence of MSU crystal deposition.[36] In the early disease stages (symptom duration <1 or 2 years), DECT sensitivity seems insufficient, owing to a weak spatial resolution precluding the detection of small deposits. A cohort study of 196 patients comparing the diagnostic performances of DECT alone according to disease duration demonstrated poor sensitivity (38%) in the very early stages (<1 year), with US providing better performance.[37] Finally, the OMERACT working group on gout suggested that DECT is superior in quantifying urate burden when compared to other modalities.[38] As a result, DECT is now included in ACR classification criteria for gout diagnosis since 2015 and in the 2023 EULAR recommendations for the imaging of crystal arthropathies.[39]

Prognostic value of DECT in gout

The first studies of the prognosis of MSU crystal deposits as measured by DECT showed that a significant volume ($\geqslant 0.81\,cm^3$) of MSU crystals in the feet was associated with a higher risk of flares in the next 6 months in 78 patients suffering from gout, whether ULT naïve or not.[34] The same conclusions were found in another study[40] where the number of flares from the past 6 months (before the inclusion in a clinical trial) was associated with the volume of crystals on DECT in patients already treated with allopurinol. Higher MSU crystal volumes may also explain the association between gout and cardiovascular comorbidities,[41,42] type 2 diabetes,[43] new CV events, and overall mortality.[35] The possibility of future flares in patients with unmeasurable MSU crystal deposition on DECT scans at baseline, particularly in patients naïve to ULT, is poorly understood, and it is not known whether the initial volume of MSU crystals measured with DECT will be a predictor of the difficulty of achieving SU level targets. A French study demonstrated that DECT in gout could help to assess the severity of the disease in terms of mortality risk by showing a correlation between a higher volume of deposits detected with DECT and all-cause mortality, especially for volumes $>0.4\,cm^3$.[35]

Detection of MSU deposits beyond joints

MSU crystal deposition is not only an issue around joints but also in organs, and particularly inside the cardiovascular system, potentially explaining the increased cardiovascular risk in patients with gout, as suggested by previous histological studies.[44] DECT seemed to be a promising tool for detecting arterial plaque containing MSU deposits. Available data is however controversial, since Klauser et al., who compared coronary artery calcium (CAC) scores and cardiovascular MSU deposits detected by DECT between 59 gout patients and 47 controls, showed a higher frequency of MSU-coded plaques and CAC scores in patients with gout. A complementary cadaver study of six subjects showed evidence of arterial deposits using polarized light microscopy of deposits compatible with MSU crystals.[45] Another study from our French group examined popliteal arteries from 126 patients with gout and 26 controls, showing a similar prevalence of MSU-coded plaques between groups, and these plaques were intimately linked to the presence of calcified plaques.[46] The study also included the

follow-up study of 17 patients showing persistent MSU-coded plaques despite extensive MSU crystal dissolution in joints during ULT, except for one MSU-coded plaque, which eventually calcified. In addition, in-depth DECT characterization of MSU-coded plaques showed that their composition was not entirely consistent with MSU deposits, as higher Z_{eff} values suggested that they may be early-calcified plaques miscoded as MSU due to insufficient calcium content. To date, there is still no convincing evidence from histopathological, immunohistochemical, or imaging data that MSU crystals do deposit inside artery walls.[47] One case report of patients suffering from severe tophaceous gout suggested that DECT could reveal urate deposits in the renal medulla, but such findings need further confirmation.[48]

Monitoring of MSU crystal deposition

Uhlig et al. explored changes in DECT urate depositions during a treat-to-target strategy with ULT in 187 gout patients who had a DECT at baseline and after 1 and 2 years. This showed decreasing DECT scores at the first and second year of follow-up on the forefeet and ankles, whether or not the patients achieved the SU target.[49] Others authors have looked into the MSU crystal depletion measured by DECT in patients taking conventional ULT, but their observations were disappointing, with only very partial crystal depletion at 18 and 24 months and over 50% persistence of baseline deposits.[50,51] These results could be explained, because in studies including patients treated with allopurinol and febuxostat, baseline volumes of MSU crystals measured with DECT, which may have actually involved substantial volumes of artifacts not expected to disappear, were very small ($<0.01\,cm^3$), with a difficult-to-measure sensitivity to change.[51] In groups of patients with more significant deposits at baseline, the change in MSU crystal volume measured with DECT was more substantial and reached around 80% of depletion[49,52] in patients managed with a treat-to-target ULT approach. The kinetics of MSU crystal depletion assessed with DECT remain unpredictable, do not seem to be entirely dependent on serum urate levels, and may involve other biological factors which are currently being studied. Such studies observe a significantly greater crystal dissolution of MSU deposits measured by DECT at 12 months (−85% vs −40%) in patients achieving an SU level <5.0 mg/dl than in those achieving <6.0 mg/dl, which has been associated with incomplete crystal disappearance, without increasing the risk of flares, supporting a target SU level <5.0 mg/dl to be generalized to all gout patients with significant MSU deposits on DECT in the French guidelines. History of hypertension appears to be a factor contributing to decreased MSU crystal depletion under ULT potentially explained by the role of anti-hypertensive drugs.[53]

What do recommendations have to say about the use of DECT in gout?

The 2023 recommendations for the imaging of crystal-induced arthropathies provided a significant step forward by supporting that DECT could provide indirect proof of MSU crystal deposition, and that proof from synovial fluid analysis is not necessarily required.[3] EULAR also recognized the ability of DECT to quantify the MSU crystal deposition burden and its usefulness in assessing tophus resolution in response to ULT. It can also explore deep-seated anatomical structures and regions.[26] DECT can be used to monitor crystal deposition, with a 1-year control appearing to be a reasonable timeframe to monitor changes in gout. Repeating DECT appears useful in cases where another associated rheumatic disease is suspected or when patients are still flaring despite prolonged adherence to treat-to-target ULT or when discontinuing flare prophylaxis. DECT is also helpful in illustrating MSU deposition and could help to explain the disease to patients to improve understanding of the disease and therefore improve treatment adherence.[3]

CPPD disease

A brief reminder of how US works in CPPD and elementary lesions of CPPD

In US, CPP crystals appear as hyperechoic deposits, exhibiting an echogenicity similar to cortical bone. CPP deposits do not create acoustic shadowing in contrast to other calcium crystals, which tend to attenuate the beam at increasing concentrations.[54] This phenomenon could be caused by the three-dimensional structure of the crystals, which may result in lower acoustic impedance and thus less attenuation of the ultrasound beam.[55] In cartilage (fibro- or hyaline) and in the synovial fluid, CPP crystals present as deposits of variable size and shape, while in tendons, they appear as multiple linear deposits following tendon fibers. They classically remain fixed, and, while they

move together with the structure they are located in on dynamic scanning.[56] The definitions have been demonstrated to be of good reliability in only two joints, the knee and the wrist, and in only two structures, hyaline cartilage and fibrocartilage.

Diagnosis of CPPD disease

The gold standard for the diagnosis of CPPD disease is the identification of CPP crystals based on synovial fluid microscopic analysis,[1] which is not always available. US in patients with CPPD could reveal the presence of CPP deposits and other unspecific signs due to the inflammatory reaction induced by the crystals.

It is currently admitted that the previously reported OMERACT definitions were highly specific and sensitive for CPPD diagnosis (76% and 88%, respectively).[55] The sensitivity of these lesions increases with the number of scanned sites and also depends on the joint being examined, the knee being the most informative joint.[57,58] In a meta-analysis of diagnostic performances of US in CPPD, the sensitivity of US appeared to be 85% in the knee and 87% in the wrist, with specificity of, respectively, 91% and 87%.[59]

The most frequently involved joints in CPPD are the wrist and the knee. In the wrist CPPD deposits are frequently found in the triangular fibrocartilage complex (TFCC), in the flexor carpi radialis tendon, in the scapholunate ligament, and the volar aspect of the radiocarpal capsule.[56,60] The knee is a potential goldmine for CPP crystals detection with US, as we know this joint to be the one involved earliest and most frequently in CPPD,[61] especially on the menisci, HC, and knee tendons. CPPD, being a systemic disorder, can potentially involve every joint, and apart from wrists and knees, hips and shoulders (particularly the acromioclavicular joint) could also be frequently affected by CPPD.[62]

Like in gout, a DC sign has also been visualized by US in patients with CPPD,[63] and this finding challenged the specificity of the DC sign for gout for a time. However, the so-called DC sign in CPPD differs from the genuine DC sign observed in gout. While MSU crystals deposit at the cartilage surface, explaining the "true" DC sign observed in gout, CPP crystals deposit within the capsule or the ligaments just above the hyaline cartilage. A dynamic assessment of the joint is necessary to distinguish the "true" from the "pseudo" DC sign, as the DC sign moves together with the subchondral bone in gout, while in CPPD the pseudo-DC sign moves in an opposite direction, as the capsule/ligament slides on the cartilage.[64,65] The deposits in CPPD are not at the surface but inside the cartilage, which also differs from gout. For the diagnosis, not all joints need to be scanned, as systematic scanning of knees and wrists, as well as the target painful joint or the hips, provide near perfect diagnostic performances.[62,66]

A study compared US diagnostic performance with conventional radiography (CR) and CT, concluding that US detected CPPD with greater sensitivity than conventional CT or plain radiography in 25 patients with crystal-proven CPPD of the knee.[67]

What is recommended for the diagnosis and monitoring using US in CPPD disease?

For US, EULAR recommends scanning disease-specific target sites (i.e., knees and wrists) and symptomatic joints for all imaging techniques.[3] Ultrasound and conventional radiography are the prioritized techniques for the diagnosis of CPPD.

In CPPD, serial imaging is not recommended unless there is an unexpected change in clinical characteristics.[3] EULAR recommendations found no evidence of imaging being useful for monitoring CPPD in clinical practice. In certain cases, such as rapidly progressing symptoms, imaging may be useful to determine whether the symptoms relate to disease severity and may help to identify an additional diagnosis. Designing studies monitoring patients with calcium crystal deposition disease would be fundamental for further understanding the natural history of the disease.[3] To the best of our knowledge, there are no US studies aiming to assess deposition evolution over time. This is basically for two reasons: first, the lack of treatments for dissolution of crystals is a strong deterrent for such studies, and second, till now, there have been no validated scoring systems for CPP deposition in joints.

The OMERACT US in CPPD subgroup has recently solved the second issue. Based on OMERACT definitions of CPPD elementary lesions, a scoring system was developed to define the extent of the burden of CPPD.[68] The ultrasound scoring system evaluates the presence of CPPD in the knees (menisci and HC) and wrists (TFCC) on a scale from 0 to 3, with grade 0: no findings consistent with CPPD, grade 1: $\leqslant 3$

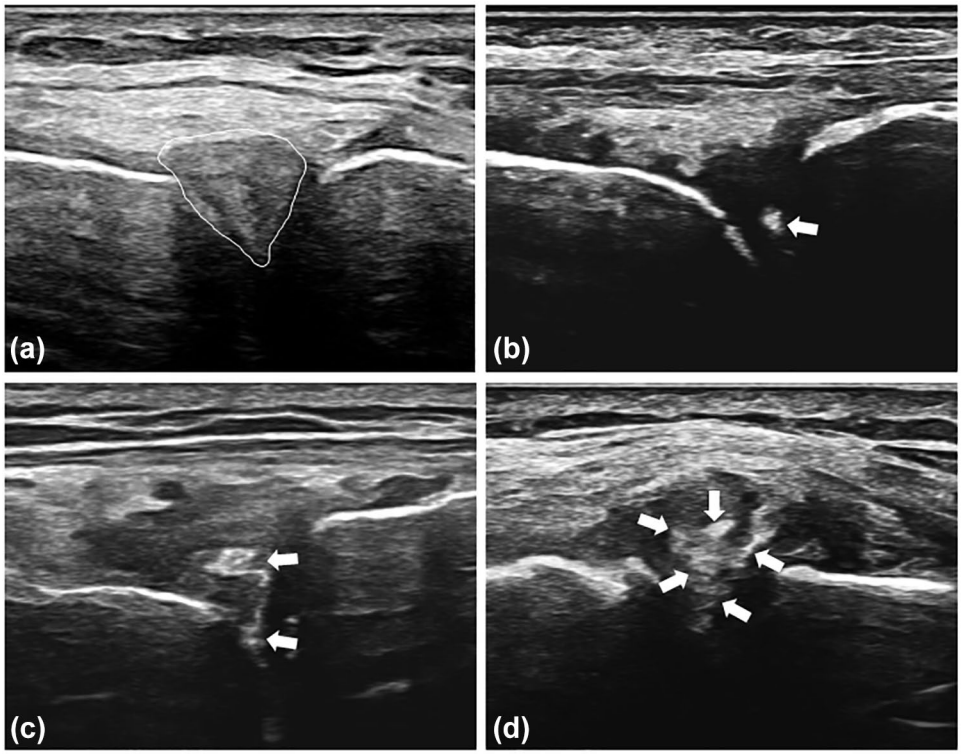

Figure 4. CPPD scoring: an example of the OMERACT CPPD scoring of the meniscus of the knee. (a) Normal meniscus without any deposition appearing as homogeneous gray triangular structure (depicted by a white continuous line). (b) The meniscus appears hypoechogenic (partially for the angle of insonation) with a bright focal deposition of CPP crystals in the middle (arrow). (c) and (d) Increasing hyperechoic deposits of CPP crystals covering less (c) and more (d) than 50% of the surface of the meniscus (arrows).
CPPD, calcium pyrophosphate deposition.

single spots or 1 small deposit, grade 2: >3 single spots or >1 small deposit or ⩾1 larger deposit occupying ⩽50% of the structure examined in the reference image, and grade 3: deposits that occupy more than 50% of the structure examined in the reference image (Figure 4). The score showed almost perfect intra- and inter-reader reliability for static images (k 0.90 and 0.84, respectively), and a substantial intra- and inter-reader reliability in patients (k 0.72 and 0.66).

The lack of treatment options has been a major obstacle for longitudinal studies on deposition changes but now for the first time, a scoring system exists that could be used to assess the natural history of the disease and potentially crystal dissolution treatments' efficacy when available.

A brief reminder of the basic principles of DECT in its application to CPPD

Use of DECT for CPPD is more complex and far less standardized than it is in gout and requires an understanding of the photoelectric effect and Compton scattering of calcium-containing structures. In addition to detecting calcifications, which conventional CT is already capable of doing, DECT needs to be able to differentiate types of calcium-containing deposits through characterization.

To characterize calcifications more efficiently, the reader needs to draw regions of interest (ROIs) manually and examine the values of five DECT parameters: CT numbers (in HU) at low (80 kV) and high (140 kV) tube potentials, the dual-energy index (DEI) calculated using the equation (attenuation low − attenuation high) divided by (attenuation low + attenuation high + 2000) applied to the ROIs, electron density (Rho), and the effective atomic number (Z_{eff}; Figure 5).[69] Using these parameters, a first in vivo study demonstrated the proof-of-concept that DECT parameters from CPP crystal deposits differed from the parameters of trabecular bone (composed of HA (hydroxyapatite)), mainly through

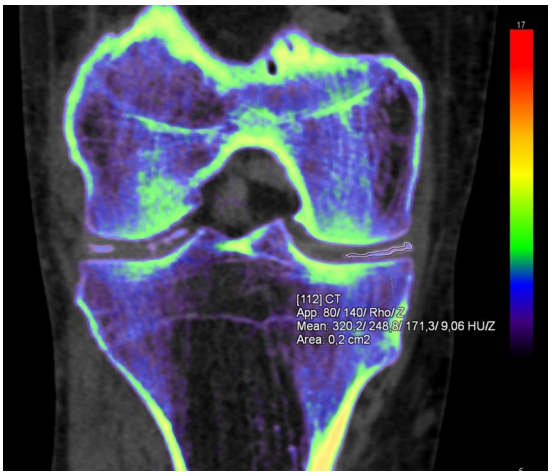

Figure 5. DECT scan of a right knee from a 78-year old woman with calcium pyrophosphate deposition disease. Images were obtained using the "Rho/Z" postprocessing settings (Siemens Syngovia). A region of interest encompassing the calcified deposition was drawn, and the software provided attenuations at 80 and 140 kV, the value of Rho (electron density) and Z_{eff} (effective atomic number).
DECT, dual-energy computed tomography.

Z_{eff} and the DEI (Figure 2). The concept was confirmed by another study comparing DECT parameters from intra-articular CPPD and basic calcium phosphate crystal deposits in tendons, all ascertained by Raman spectroscopy, and which showed that at equal density, CPP and basic calcium phosphate (BCP) deposits differed in DEI and Z_{eff} parameters, but with a significant overlap of values, suggesting that DECT would not be sufficiently reliable in clinical practice to efficiently distinguish between CPP and BCP deposits.[69,70]

Diagnostic performances of DECT in CPPD

The diagnostic performance of DECT in detecting CPP crystal deposits in comparison with conventional radiography has been studied in human knees at the time of total knee arthroplasty.[71] DECT was far more sensitive (90% vs 49%) and slightly less specific than conventional radiography and had an overall diagnostic accuracy for CPP deposition in the same range as conventional CT.[72,73] These differences in diagnostic performances versus conventional radiography are explained by the fact that CT can detect smaller calcified deposits, which have a higher probability of being composed only of BCP crystals than large deposits detected by radiography which contain at least some CPP crystals, and therefore has the highest specificity. After the proof of concept demonstrated that DECT could provide some specific characterization of CPP deposits through their biochemical signature, it was hypothesized that DECT could detect meniscal biochemical changes before CPP deposits could be observed on CT images. A study explored this hypothesis, but showed that DECT could differentiate calcified meniscal ROIs in CPPD patients with visible calcifications from ROIs in controls, but failed to significantly distinguish between ROIs from patients with CPPD without visible calcification and controls. Also, DEI values increased in menisci with presumed early CPPD.[73] To date, the proof of concept that DECT can aid in the characterization of CPPD has been demonstrated, but in a clinical setting, it is insufficiently efficient in differentiating them from other calcium-containing deposits. DECT does not provide significant additional information compared to conventional CT for the diagnosis of CPPD. Its role is limited to improving detection in certain regions along with normal conventional radiographs and when synovial fluid aspiration is difficult, or in the spine, or in the context of research to provide a better understanding of the pathogenic role of CPP crystals, particularly in osteoarthritis.[69] Postprocessing tools to quantify CPPD may add another role for DECT in the future, but none have been validated yet.[74] These advances made with DECT have paved the way for photon-counting CTs, which will have increased characterization abilities with higher spatial resolution. Tedeschi et al. discussed a novel definition for the appearance of CPPD on DECT and CT. On conventional CT, CPPD is defined as linear or punctate calcification less dense (in contract to BCP deposits, which are generally larger, denser, and "cloudlike") than cortical bone, located within fibro or hyaline articular cartilage, synovial membrane, the joint capsule, or tendons. The absolute number of HU used to differentiate CPPD from BCP was removed from the definition for several reasons including the fact that CT numbers of calcifications depend on the CT acquisition protocol. On DECT, the same definition could be applied but calcifications must have a DEI between 0.016 and 0.036.[74]

What is recommended for the use of DECT in CPPD disease?

CPPD disease is typically characterized by intermittent acute episodes of inflammation, but it can also manifest as chronic arthropathies, which are more challenging to diagnose. DECT could help to identify CPPD in those particular forms providing quantitative assessment of crystal deposition.[1] DECT should be performed as a priority on the knees and wrists, which are disease-specific target sites, and also on symptomatic areas. It is important to note that crystal aggregates or crystal deposits identified on DECT do not always lead to clinical manifestations. The first imaging techniques recommended by EULAR in the diagnosis of CPPD remain CR, US, and conventional CT if axial involvement is suspected, with DECT potentially being used to identify crystal deposition in cases of difficult diagnosis.

The potential of DECT was acknowledged in the 2023 ACR/EULAR classification criteria for CPPD disease among advanced techniques able to provide evidence of CPPD, together with US and conventional CT.[1] Due to its good negative predictive value, this exam is able to make CPPD disease improbable when DECT does not identify significant crystal deposition.

Perspectives

Advances in the detection of calcium and MSU crystal deposits are expected in the future with the emergence of multienergy spectral photon-counting CT (SPCCT), which offers increased 3D spatial resolution around 100 µm with less partial volume effects and with lower energy ranges.[75,76] Multienergy SPCCT is a novel imaging technique that uses a standard polychromatic X-ray source and photon counting detector that records the number and energy of transmitted photons in multiple energy bins.[77] As X-ray attenuation of each material is energy dependent, multienergy bin data allow specific identification and quantification of several materials simultaneously.[75] Some studies have found that SPCCT imaging can differentiate between MSU, CPP, and HA in vitro.[78,76] Not only is SPCCT able to detect and differentiate MSU but it can also distinguish CPP crystals from HA aggregates far more precisely that DECT. This highlights that SPCCT has potential advantages over DECT in detecting and characterizing MSU crystal deposits (showing finer details and a higher MSU volume, probably due to better sensitivity and a higher spatial resolution) and that it could distinguish crystal aggregates, reflecting the potential usefulness of multienergy SPCCT in the diagnosis of crystal arthropathies.

Conclusion

Diagnosis of crystal arthropathies have experienced a lot of change since last years, especially with the development of imaging allowing to obtain noninvasive crystal-proof even when synovial fluid aspiration is not available. DECT and US are the most used advanced imaging techniques in crystal arthropathies and their role extends beyond diagnosis to assess the prognosis and are increasingly used to guide the management of crystal arthropathies (Table 1).

Table 1. Key publications in advanced techniques (ultrasound and DECT in gout and CPPD disease).

Study type	Gout	CPPD disease
Proof-of-concept study ultrasound	Grassi et al.[5]	Grassi et al.[5]
Proof-of-concept study DECT	Choi et al.[6]	Pascart et al.[69]
Diagnostic performances ultrasound	Lee and Song[11]	Cipolletta et al.[59]
Diagnostic performances DECT	Gruber et al.[31]	
Quantification of crystal burden ultrasound	Christiansen et al.[18]	Sirotti et al.[68]
Quantification of crystal burden DECT	Pascart et al.[23]	Not done.
Classification criteria integrating ultrasound and DECT	Neogi et al.[2]	Abhishek et al.[1]
Imaging recommendations for the use of ultrasound and DECT	Mandl et al.[3]	Mandl et al.[3]

CPPD, calcium pyrophosphate deposition; DECT, dual-energy computed tomography.

Declarations

Ethics approval and consent to participate
Not applicable.

Consent for publication
Not applicable.

Author contributions
Victor Laurent: Conceptualization; Formal analysis; Investigation; Writing – original draft.

Georgios Filippou: Conceptualization; Methodology; Supervision; Validation; Visualization; Writing – original draft; Writing – review & editing.

Silvia Sirotti: Formal analysis; Investigation; Resources; Visualization; Writing – review & editing.

Tristan Pascart: Conceptualization; Data curation; Formal analysis; Methodology; Project administration; Validation; Visualization; Writing – original draft; Writing – review & editing.

Acknosewledgements
None.

Funding
The authors received no financial support for the research, authorship, and/or publication of this article.

Competing interests
V.L. has no conflicts of interests. T.P. received honorary fees from Novartis and research grants from Horizon Pharmaceuticals (Amgen). S.S. has no conflict of interest. G.F. has received research grant from Eli Lilly for studies on CPPD.

Availability of data and materials
Not applicable.

ORCID iDs
Victor Laurent https://orcid.org/0009-0007-8081-0095

Tristan Pascart https://orcid.org/0000-0002-8395-826X

References
1. Abhishek A, Tedeschi SK, Pascart T, et al. The 2023 ACR/EULAR classification criteria for calcium pyrophosphate deposition disease. *Ann Rheum Dis* 2023; 82(10): 1248–1257.
2. Neogi T, Jansen TLTA, Dalbeth N, et al. 2015 Gout classification criteria: an American College of Rheumatology/European League Against Rheumatism collaborative initiative. *Ann Rheum Dis* 2015; 74(10): 1789–1798.
3. Mandl P, D'Agostino MA, Navarro-Compán V, et al. 2023 EULAR recommendations on imaging in diagnosis and management of crystal-induced arthropathies in clinical practice. *Ann Rheum Dis* 2024; 83(6): 752–729.
4. Sirotti S, Becce F, Sconfienza LM, et al. Reliability and diagnostic accuracy of radiography for the diagnosis of calcium pyrophosphate deposition: performance of the novel definitions developed by an international multidisciplinary working group. *Arthritis Rheumatol* 2023; 75(4): 630–638.
5. Grassi W, Meenagh G, Pascual E, et al. "Crystal Clear"—sonographic assessment of gout and calcium pyrophosphate deposition disease. *Semin Arthritis Rheum* 2006; 36(3): 197–202.
6. Choi HK, Al-Arfaj AM, Eftekhari A, et al. Dual energy computed tomography in tophaceous gout. *Ann Rheum Dis* 2009; 68(10): 1609–1612.
7. Liu E, Dalbeth N, Pool B, et al. Ultrasound findings of monosodium urate aggregates in patients with gout. *Gout Urate Cryst Depos Dis* 2023; 1(2): 83–88.
8. Bruyn GA, Iagnocco A, Naredo E, et al. OMERACT definitions for ultrasonographic pathologies and elementary lesions of rheumatic disorders 15 years on. *J Rheumatol* 2019; 46(10): 1388–1393.
9. Terslev L, Gutierrez M, Christensen R, et al. Assessing elementary lesions in gout by ultrasound: results of an OMERACT patient-based agreement and reliability exercise. *J Rheumatol* 2015; 42(11): 2149–2154.
10. Filippucci E, Cipolletta E, Sirotti S, et al. Optimising the use of ultrasound in gout: a review from the ground up. *Gout Urate Cryst Depos Dis* 2024; 2(2): 86–100.
11. Lee YH and Song GG. Diagnostic accuracy of ultrasound in patients with gout: a meta-analysis. *Semin Arthritis Rheum* 2018; 47(5): 703–709.
12. Gessl I, Sakellariou G, Wildner B, et al. Systematic literature review to inform the EULAR recommendations for the use of imaging in crystal-induced arthropathies in clinical practice. *Ann Rheum Dis* 2024; 83(9): 1208–1224.
13. Thiele RG and Schlesinger N. Ultrasonography shows disappearance of monosodium urate crystal deposition on hyaline cartilage after sustained normouricemia is achieved. *Rheumatol Int* 2010; 30(4): 495–503.

14. Ottaviani S. Imaging follow-up of MSU crystal depletion. *Gout Urate Cryst Depos Dis* 2024; 2(1): 34–44.
15. Christiansen SN, Østergaard M, Slot O, et al. Assessing the sensitivity to change of the OMERACT ultrasound structural gout lesions during urate-lowering therapy. *RMD Open* 2020; 6(1): e001144.
16. Ebstein E, Forien M, Norkuviene E, et al. Ultrasound evaluation in follow-up of urate-lowering therapy in gout: the USEFUL study. *Rheumatology* 2019; 58(3): 410–417.
17. Ebstein E, Forien M, Norkuviene E, et al. UltraSound evaluation in follow-up of urate-lowering therapy in gout phase 2 (USEFUL-2): duration of flare prophylaxis. *Joint Bone Spine* 2020; 87(6): 647–651.
18. Christiansen SN, Filippou G, Scirè CA, et al. Consensus-based semi-quantitative ultrasound scoring system for gout lesions: results of an OMERACT Delphi process and web-reliability exercise. *Semin Arthritis Rheum* 2021; 51(3): 644–649.
19. Hammer HB, Karoliussen L, Terslev L, et al. Ultrasound shows rapid reduction of crystal depositions during a treat-to-target approach in gout patients: 12-month results from the NOR-Gout study. *Ann Rheum Dis* 2020; 79(11): 1500–1505.
20. Bardin T, Letavernier E and Correas JM. The gouty kidney: a reappraisal. *Gout Urate Cryst Depos Dis* 2023; 1(1): 25–36.
21. Carotti M, Salaffi F, Beci G, et al. The application of dual-energy computed tomography in the diagnosis of musculoskeletal disorders: a review of current concepts and applications. *Radiol Med (Torino)* 2019; 124(11): 1175–1183.
22. Pascart T and Budzik JF. Dual-energy computed tomography in crystalline arthritis: knowns and unknowns. *Curr Opin Rheumatol* 2022; 34(2): 103–110.
23. Pascart T, Grandjean A, Norberciak L, et al. Ultrasonography and dual-energy computed tomography provide different quantification of urate burden in gout: results from a cross-sectional study. *Arthritis Res Ther* 2017; 19(1): 171.
24. Parakh A, An C, Lennartz S, et al. Recognizing and minimizing artifacts at dual-energy CT. *Radiographics* 2021; 41: E96.
25. Christiansen SN, Müller FC, Østergaard M, et al. Dual-energy CT in gout patients: do all colour-coded lesions actually represent monosodium urate crystals? *Arthritis Res Ther* 2020; 22: 212.
26. Richette P, Doherty M, Pascual E, et al. 2018 updated European League Against Rheumatism evidence-based recommendations for the diagnosis of gout. *Ann Rheum Dis* 2020; 79(1): 31–38.
27. Stewart S, Gamble G, Doyle AJ, et al. The statistical challenge of analysing changes in dual energy computed tomography (DECT) urate volumes in people with gout. *Semin Arthritis Rheum* 2023; 63: 152303.
28. Laurent V, Jauffret C, Ducoulombier V, et al. Are gout patients with negative dual-energy computed tomography for monosodium urate crystal deposition easy to treat? *Rheumatology* 2024; keae061.
29. Døssing A, Müller FC, Becce F, et al. Dual-energy computed tomography for detection and characterization of monosodium urate, calcium pyrophosphate, and hydroxyapatite: a phantom study on diagnostic performance. *Invest Radiol* 2021; 56(7): 417–424.
30. Choi HK, Burns LC, Shojania K, et al. Dual energy CT in gout: a prospective validation study. *Ann Rheum Dis* 2012; 71(9): 1466–1471.
31. Gruber M, Bodner G, Rath E, et al. Dual-energy computed tomography compared with ultrasound in the diagnosis of gout. *Rheumatology (Oxford)* 2014; 53: 173–179.
32. Shang J, Zhou LP, Wang H, et al. Diagnostic performance of dual-energy CT versus ultrasonography in gout: a meta-analysis. *Acad Radiol* 2022; 29(1): 56–68.
33. Neogi T, Jansen TL, Dalbeth N, et al. 2015 Gout classification criteria: an American College of Rheumatology/European League Against Rheumatism collaborative initiative. *Ann Rheum Dis* 2015; 74(10): 1789–1798. (Erratum in: *Ann Rheum Dis* 2016; 75(2): 473.)
34. Yu Z, Mao T, Xu Y, et al. Diagnostic accuracy of dual-energy CT in gout: a systematic review and meta-analysis. *Skeletal Radiol* 2018; 47(12): 1587–1593.
35. Pascart T, Grandjean A, Capon B, et al. Monosodium urate burden assessed with dual-energy computed tomography predicts the risk of flares in gout: a 12-month observational study: MSU burden and risk of gout flare. *Arthritis Res Ther* 2018; 20(1): 210.
36. Marty-Ané A, Norberciak L, Andrès M, et al. Crystal deposition measured with dual-energy computed tomography: association with mortality and cardiovascular risks in gout. *Rheumatology (Oxford)* 2021; 60(10): 4855–4860.
37. Singh JA, Budzik JF, Becce F, et al. Dual-energy computed tomography versus ultrasound,

alone or combined, for the diagnosis of gout: a prospective study of accuracy. *Rheumatology (Oxford)* 2021; 60: 4861–4867.

38. Shang J, Li XH, Lu SQ, et al. Gout of feet and ankles in different disease durations: diagnostic value of single-source DECT and evaluation of urate deposition with a novel semi-quantitative DECT scoring system. *Adv Rheumatol* 2021; 61: 36.
39. Grainger R, Dalbeth N, Keen H, et al. Imaging as an outcome measure in gout studies: report from the OMERACT Gout Working Group. *J Rheumatol* 2015; 42(12): 2460–2464.
40. FitzGerald JD, Dalbeth N, Mikuls T, et al. 2020 American College of Rheumatology guideline for the management of gout. *Arthritis Care Res* 2020; 72(6): 744–760.
41. Dalbeth N, Becce F, Botson JK, et al. Dual-energy CT assessment of rapid monosodium urate depletion and bone erosion remodelling during pegloticase plus methotrexate co-therapy. *Rheumatology* 2022; 61(12): 4898–4904.
42. Liu-Bryan R, Guo T, Lee J, et al. Atherogenic activation of human vascular smooth muscle cells by monosodium urate crystals. *Gout Urate Cryst Depos Dis* 2023; 1(3): 192–207.
43. Andrés M. Gout and cardiovascular disease: mechanisms, risk estimations, and the impact of therapies. *Gout Urate Cryst Depos Dis* 2023; 1(3): 152–166.
44. Pascart T, Ramon A, Ottaviani S, et al. Association of specific comorbidities with monosodium urate crystal deposition in urate-lowering therapy-naive gout patients: a cross-sectional dual-energy computed tomography study. *J Clin Med* 2020; 9(5): 1295.
45. Park JJ, Roudier MP, Soman D, et al. Prevalence of birefringent crystals in cardiac and prostatic tissues, an observational study. *BMJ Open* 2014; 4: e005308.
46. Klauser AS, Halpern EJ, Strobl S, et al. Dual-energy computed tomography detection of cardiovascular monosodium urate deposits in patients with gout. *JAMA Cardiol* 2019; 4(10): 1019–1028.
47. Pascart T, Carpentier P, Choi HK, et al. Identification and characterization of peripheral vascular color-coded DECT lesions in gout and nongout patients: the VASCURATE study. *Semin Arthritis Rheum* 2021; 51: 895–902.
48. Pascart T and Budzik JF. Does monosodium urate crystal vascular deposition exist? Review of the evidence. *Gout Urate Cryst Depos Dis* 2023; 1(3): 208–216.
49. Bardin T, Tran KM, Nguyen QD, et al. Renal medulla in severe gout: typical findings on ultrasonography and dual-energy CT study in two patients. *Ann Rheum Dis* 2019; 78(3): 433–434.
50. Uhlig T, Eskild T, Karoliussen LF, et al. Two-year reduction of dual-energy CT urate depositions during a treat-to-target strategy in gout in the NOR-Gout longitudinal study. *Rheumatology* 2022; 61(SI): SI81–SI85.
51. Dalbeth N, Billington K, Doyle A, et al. Effects of allopurinol dose escalation on bone erosion and urate volume in gout: a dual-energy computed tomography imaging study within a randomized, controlled trial. *Arthritis Rheumatol* 2019; 71(10): 1739–1746.
52. Ellmann H, Bayat S, Araujo E, et al. Effects of conventional uric acid–lowering therapy on monosodium urate crystal deposits. *Arthritis Rheumatol* 2020; 72(1): 150–156.
53. Uhlig T, Eskild T, Karoliussen LF, et al. Two-year reduction of dual-energy CT urate depositions during a treat-to-target strategy in gout in the NOR-Gout longitudinal study. *Rheumatology* 2022; 61(SI): SI81–SI85.
54. Chen L, Gamble GD, Horne A, et al. Changes in tophus composition during urate-lowering therapy: a dual-energy computed tomography study. *Arthritis Care Res (Hoboken)* 2023; 75(9): 1949–1954.
55. Laurent V, Jauffret C, Pacaud A, et al. Factors influencing the kinetics of MSU crystal depletion measured with dual-energy CT in patients with gout. *RMD Open* 2023; 9(4): e003725.
56. Filippou G, Sirotti S, Cipolletta E, et al. Optimizing the use of ultrasound in calcium pyrophosphate deposition (CPPD): a review from the ground up. *Gout Urate Cryst Depos Dis* 2024; 2(1): 17–33.
57. Filippou G, Scanu A, Adinolfi A, et al. Criterion validity of ultrasound in the identification of calcium pyrophosphate crystal deposits at the knee: an OMERACT ultrasound study. *Ann Rheum Dis* 2021; 80(2): 261–267.
58. Filippou G, Scirè CA, Adinolfi A, et al. Identification of calcium pyrophosphate deposition disease (CPPD) by ultrasound: reliability of the OMERACT definitions in an extended set of joints—an international multiobserver study by the OMERACT calcium pyrophosphate deposition disease ultrasound subtask force. *Ann Rheum Dis* 2018; 77: 1195–1200.
59. Sakellariou G, Scirè CA, Adinolfi A, et al. Differential diagnosis of inflammatory

arthropathies by musculoskeletal ultrasonography: a systematic literature review. *Front Med* 2020; 7: 141.

60. Filippou G, Adinolfi A, Iagnocco A, et al. Ultrasound in the diagnosis of calcium pyrophosphate dihydrate deposition disease. A systematic literature review and a meta-analysis. *Osteoarthritis Cartilage* 2016; 24(6): 973–981.
61. Cipolletta E, Filippou G, Scirè CA, et al. The diagnostic value of conventional radiography and musculoskeletal ultrasonography in calcium pyrophosphate deposition disease: a systematic literature review and meta-analysis. *Osteoarthritis Cartilage* 2021; 29(5): 619–632.
62. Cipolletta E, Di Matteo A, Smerilli G, et al. Ultrasound findings of calcium pyrophosphate deposition disease at metacarpophalangeal joints. *Rheumatology (Oxford)* 2022; 61(10): 3997–4005.
63. Adinolfi A, Sirotti S, Sakellariou G, et al. Which are the most frequently involved peripheral joints in calcium pyrophosphate crystal deposition at imaging? A systematic literature review and meta-analysis by the OMERACT ultrasound—CPPD subgroup. *Front Med* 2023; 10: 1131362.
64. Cipolletta E, Moscioni E, Sirotti S, et al. Diagnosis of calcium pyrophosphate crystal deposition disease by ultrasonography: how many and which sites should be scanned? *Rheumatology* 2024; 63(8): 2205–2212.
65. Adinolfi A, Picerno V, Di Sabatino V, et al. Inquiry is fatal to certainty—is the ultrasonography double contour sign specific for uric acid-induced arthritis? *Arthritis Rheum* 2013; 65(7): 1952.
66. Cipolletta E, Abhishek A, Di Matteo A, et al. Dynamic assessment of the double contour sign by ultrasonography helps to distinguish between gout and calcium pyrophosphate deposition disease. *RMD Open* 2023; 9(1): e002940.
67. Filippou G, Miguel-Pérez M, Coronel L, et al. The ultrasonographic pseudo-double contour sign in calcium pyrophosphate deposition disease: an anatomic explanation and how to distinguish it from gout. *Arthritis Rheumatol* 2023; 75(4): 639–640.
68. Cipolletta E, Moscioni E, Sirotti S, et al. Diagnosis of calcium pyrophosphate crystal deposition disease by ultrasonography: how many and which sites should be scanned? *Rheumatology (Oxford)* 2024; 63(8): 2205–2212.
69. Cipolletta E, Filippucci E, Abhishek A, et al. In patients with acute mono/oligoarthritis, a targeted ultrasound scanning protocol shows great accuracy for the diagnosis of gout and CPPD. *Rheumatology* 2023; 62(4): 1493–1500.
70. Barskova VG, Kudaeva FM, Bozhieva LA, et al. Comparison of three imaging techniques in diagnosis of chondrocalcinosis of the knees in calcium pyrophosphate deposition disease. *Rheumatology (Oxford)* 2013; 52: 1090–1094.
71. Sirotti S, Terslev L, Filippucci E, et al. Development and validation of an OMERACT ultrasound scoring system for the extent of calcium pyrophosphate crystal deposition at the joint level and patient level. *Lancet Rheumatol* 2023; 5: e474–e482.
72. Pascart T, Norberciak L, Legrand J, et al. Dual-energy computed tomography in calcium pyrophosphate deposition: initial clinical experience. *Osteoarthritis Cartilage* 2019; 27(9): 1309–1314.
73. Pascart T, Falgayrac G, Norberciak L, et al. Dual-energy computed-tomography-based discrimination between basic calcium phosphate and calcium pyrophosphate crystal deposition *in vivo*. *Ther Adv Musculoskelet Dis* 2020; 12: 1759720X20936060.
74. Tanikawa H, Ogawa R, Okuma K, et al. Detection of calcium pyrophosphate dihydrate crystals in knee meniscus by dual-energy computed tomography. *J Orthop Surg Res* 2018; 13(1): 73.
75. Misra D, Guermazi A, Sieren JP, et al. CT imaging for evaluation of calcium crystal deposition in the knee: initial experience from the Multicenter Osteoarthritis (MOST) study. *Osteoarthritis Cartilage* 2015; 23(2): 244–248.
76. Budzik J, Marzin C, Legrand J, et al. Can dual-energy computed tomography be used to identify early calcium crystal deposition in the knees of patients with calcium pyrophosphate deposition? *Arthritis Rheumatol* 2021; 73(4): 687–692.
77. Pascart T, Norberciak L, Legrand J, et al. Dual-energy computed tomography in calcium pyrophosphate deposition: initial clinical experience. *Osteoarthritis Cartilage* 2019; 27(9): 1309–1314.
78. Tedeschi SK, Becce F, Pascart T, et al. Imaging features of calcium pyrophosphate deposition disease: consensus definitions from an international multidisciplinary working group. *Arthritis Care Res* 2023; 75(4): 825–834.